Chalcogenide Letters Vol. 20, No. 4, April 2023, p. 261 - 276

Exceptional and innovational analysis of n-CdS/p-Si solar cells based on software packages and bias point models: insights into theoretical and experimental characteristics of fabricated solar cells

A. A. Hassan[a,b], S. Y. Al-Nami[a], H. A. Alrafai[a], E. Al-Amery[c], E. R. Shaaban[d], A. Qasem[e*]

[a]*Department of Chemistry, Faculty of Science, King Khalid University, Abha, Saudi Arabia.*

[b]*Department of Chemistry, Faculty of Science for Girls, Ain Shams University, Cairo, Egypt.*

[c]*Department of Microbiology, Faculty of Applied Science, Taiz University, Taiz 6350, Yemen*

[d]*Department of physics, Faculty of Science, Al-Azhar University, Assiut, 71542, Egypt.*

[e]*Department of Physics, Faculty of Science, Al-Azhar University, Nasr City 11884, Cairo, Egypt.*

The characteristics of a single solar cell made by CdS thin film deposition on a silicon glass substrate were estimated using simulation models in this study. An aluminum electrode was attached to a silicon wafer to produce a heterojunction, and the indium fingers were fashioned into another electrode and connected directly to the CdS layer. Simulation steps were performed using PV*SOL 3.0 software package and bias points (I_{SC}, V_{OC}) models. In addition to the use of advanced programs such as MATLAB software (Shell SQ150 PV module), Mathcad 2000 program, and Origin Lab 2019 program.Simulation programs for extracting photovoltaic parameters have been executed together with the laboratory procedures. The simulation programs and experimental procedures aimed in general to know the (current-voltage) and (power-voltage) characteristics of the studied single-diode photovoltaic.

(Received January 18, 2023; Accepted April 7, 2023)

Keywords: Simulation programs, Photovoltaic cells, Solar cells, Solar irradiance, CdS/Si heterojunction

1. Introduction

A single diode model (SDM) is usually utilized to model photovoltaic PV modules, including *(I-V)* and (*P-V*) characteristics of conventional modules [1]. The utilized equations to describe the existing simulation models are transcendental, namely, supernatural in principle, and typically entail substantial mathematical complexity in their solutions, and thus they may involve many assumptions and approximations to simple them [2, 3].

As solar radiation and temperature affected the (*I-V*) and (*P-V*) characteristics of solar cells, and they are constantly changing, the dilemma of modeling photovoltaic systems is increasing [2-4].

The PV data sheet normally only gives the system parameters when the standardized test conditions, (STC), namely, the temperature of the PV cell, T_c and solar irradiance, Ψ equal to $25\ ^oC$ and $1000\, w\ /\ m^2$, respectively. Therefore, in STC, the parameters needed to model PV modeling are derived, and such parameters should be modified depending on the existing temperature and solar radiation [4].

* Corresponding author: alkhteebammar36@yahoo.com
https://doi.org/10.15251/CL.2023.204.261

On the other hand, analysis and simulation work (mentioned experimental results) is typically to calculate the studied hypothesis of importance and then reproduce it. A comparable circuit similar to the system to be characterized can describe the characteristics of PV solar cells and modules. For specific systems, there are more or less structured models that are utilized to simulate the characteristics of photovoltaic systems (*I-V*) based on conditions such as solar irradiance and temperature [5]. In CdS semiconductors, there are great efforts and various works. The optical, thermal and electrical aspects of CdS semiconductor were studied [6-13].

The current work aims to extract the parameters of the photovoltaic cell under study using simulation modeling methods and experimental procedures. Our current work provides also a theoretical preface to the equations used in the simulation programs to understand the nature of the programs and the parameters that make up it. The purpose of applying the simulation programs and the experimental procedures is to finally obtain the (current-voltage) and (power-voltage) characteristic curves of the CdS/Si solar cell. In addition to applying simulation modeling under conditions different from standard conditions, the simulation model is also applied to standard test conditions represented by the absolute temperature of the diode, $T_c = 25\ ^oC$ and the solar irradiance, $\psi = 1000\, w\ / m^2$.

2. Experimental methods

The CdS film's thickness is (120 *nm*), which was measured using a quartz crystal monitor (FTM4, Edwards). The film was prepared by the thermal evaporation method utilizing a high vacuum coating unit. (Edwards, E306A, $4\times10^{-4}\ Torr$) onto p-type (1 0 0) silicon single crystal substrate (270 μm) which was cleaned in pure alcohol and distilled water for 5 *min*. after etching, the silicon wafer. P-type silicon was formed using doping of silicon with $2\times10^{15}\ cm^{-3}$ boron gas to transform it into a conducting material that rapidly takes voltage as it was applied. The surface of the Si-substrate was first handled with a cathodic protection 4, CP_4 buffer etching solution (HF: HNO3: CH_3COOH) in the corresponding ratios (1:6:1) for time-periodic (2 *min*) to eliminate the surface film of silicon dioxide, SiO_2 [14]. Then, the heterojunction device of n-CdS/p-Si solar cell was fabricated. The initial ohmic contact was made by depositing indium fingers (In) in the form of a translucent mesh on the surface of the CdS film. The other ohmic contact, which was aluminum element Al, was formed on the reverse of the silicon substrate. For small voltages, these contacts are considered ohmic [15]. The conventional circuits (Keithley 610 and 617 as voltage sources and ammeters) were used to measure the current and voltage in the generated device. The dark current-voltage characteristics were observed in a completely dark room at 298 K, but for measurements performed at higher temperatures, the operation was performed in a dark furnace. The thermocouple (NiCr-NiAl) is connected to a digital thermometer to measure the temperature of the sample. The thickness of In and Al electrodes were 50 and 100 *nm*, respectively. The well-known "Edwards-E306A" coating device is equipped with a quartz crystal monitor (FTM4, Edwards, UK), which was used to monitor and control the deposition rate and simultaneously measure the thickness of the mentioned film. To extract the studied single diode parameters, simulation programs were the software packages (PV*SOL 3.0), bias points modes, and other programs that have been used to perform the calculations and the graph were MATLAB software (Shell SQ150 PV module), Mathcad 2000 program and Origin Lab 2019 program.

3. Foreword and theoretical description

3.1. General descriptive model for simulating solar cell data

According to the output current, I_{out} of the photovoltaic cell or the output voltage, V_{out} of the photovoltaic cell, the characteristics of the photovoltaic cell affected by solar radiation are summarized.

As common, a description model for a single diode and other description models for a dual diode. These are two simulation models commonly used in practice among several descriptive simulation models that express the current-voltage characteristics of the solar cell [16]. The simulation model of the very simple parabolic circuit of the solar cell is represented by an explanatory diagram that is easy to implement in practice so that it is highly compatible with the electrical performance of the actual solar cell. In this description diagram, (see Fig.1), it is obvious that the solar cell diode model consists of series resistance and parallel resistance (parasitic resistance), as well as diodes and current sources [17]. The model representing the concept of Fig. 1 is called a general model of photovoltaic cells in the single diode model. The model has five parameters we will mention later.

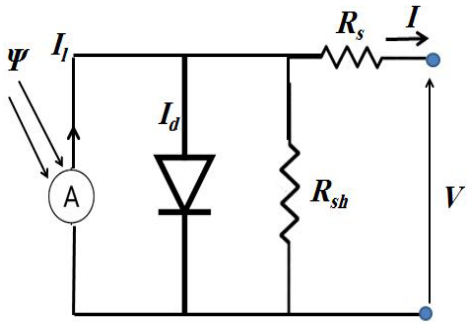

Fig. 1. A general model of photovoltaic cells (with five parameters) in the single diode model.

Based on Fig. 1, the total photovoltaic current I is mathematically expressed in a basic equation according to Kirchhoff's first law as follows [16, 17]:

$$\sum_{i}^{u} I_{in} = \sum_{i}^{u} I_{out} \tag{1}$$

Thus:

$$I = I_l - I_{sh} - I_d \tag{2}$$

Here: I is the total current of the circuit, I_l is the light generated current, I_{sh} is the shunt current, and I_d represents the diode current. The current unit is the international unit (amps).

It is known that [16, 17]:

$$I_{sh} = \left(\frac{V + IR_S}{R_{sh}} \right) \tag{3}$$

$$I_d = I_0 \times \left(\exp\left(\frac{V + IR_S}{N_s V_{th}} \right) - 1 \right) \tag{4}$$

$$V_{th} = (\frac{nk_B T_c}{q}) = 25.7\ mV \ \ (at\ 25\ ^oC) \tag{5}$$

where$V$,is saturation current I_0 is the source's voltaic,the number of photovoltaic module is N_S cells connected in series (in our work, is the shuntR_{sh} , is the series resistanceR_S), $N_S = 1$ resistance, k_B is Boltzmann's constant ($k_B = (1.38 \times 10^{-23}\ J/K)$), q is an electronic charge ($1.6 \times 10^{-19}\ C$), T_c is the absolute temperature of the diode, represents a parameter depends on n the material of the diode (or so-called diode quality factor and it without unit) and V_{th} is the thermal voltage. Now, one can express the total current that passes in the circuit (see Fig. 1) as follows [16, 17]:

$$I = I_l - \left(\frac{V + IR_S}{R_{sh}} \right) - I_0 \times \left(\exp\left(\frac{V + IR_S}{N_s V_t} \right) - 1 \right) \tag{6}$$

According to this descriptive model, the problem of defining model parameters is limited to two external parameters, namely, I_l and I_0, and also the three descriptive internal parameters are n , R_s and R_{sh}, which equal to five parameters.

3.2. External parameters(I_l and I_0) for solar cell

3.2.1. The light generated current, I_l

The generated current by light is mathematically expressed as [16. 17]:

$$I_l = \left(\frac{\Psi}{\Psi^*} \right) \left(I_l^* + \Phi_i [T_C - T_C^*] \right) \tag{7}$$

Here:

$$I_l^* = I_{SC}^* \tag{8}$$

$$\Phi_i = \left(\frac{I_{SC} - I_{SC}^*}{T_C - T_C^*} \right) \tag{9}$$

where, superscript * illustrates the value with reference conditions ($T_C = 25^oC$ and $\Psi = 1\ kWh/m^2$), Ψ is solar irradiance, I_{SC} is short circuit current, and Φ_i is the short-circuit current temperature of the solar cell coefficient in unit (A/K).

3.2.2. The saturation current of the cell (I_0)

$$I_0 = I_0^* \left(\frac{T_C^*}{T_C} \right)^3 . \exp\left(\frac{qE_g}{nk_B} \left(\frac{T_C - T_C^*}{T_C T_C^*} \right) \right) \tag{10}$$

$$I_0^* = I_{SC}^* . (\exp\left(\frac{V_{OC}^*}{V_{th}^*} \right) - 1) \tag{11}$$

Here, T_C^* is the reference temperature of the PV cell, is the reference thermalwhich V_{th}^* voltage of the cell, and I_{SC}^* is the reference short current of the cell.

The parallel resistance in the diode hetero-junction represents so-called shunt resistance. This resistance may mainly appear on the entire surface of the actual solar cell system. Leakage current occurs at the p-n junction or even at the grain size of the border (in reality, the leakage current seems to be parallel resistance). On the other hand, all voltage drops between the main propagation resistance of the solar cell and the load can be overcome by series resistance (actually, series resistance represents the inner resistance of the flowing current). Here, the damages attributed to the resistance inserted in the adhere joints of solar cells, emitter device and base areas, cell metallization, and cell interconnection busbars will all have an impact reach the value of R_s [3].

In order to simplify the model, in the case of a single diode, we can give the following parasitic resistance data (series resistance, R_s and parallel (shunt) resistance, respectively) [16-18]:

$$R_s = \left(\frac{\partial V}{\partial I} \right)_{V=0} = 0 \tag{12}$$

$$R_{sh} = \left(\frac{\partial V}{\partial I} \right)_{I=0} = \infty \tag{13}$$

And also:

The quality factor of a single diode is equal to 1 (although it is a parameter related to the type of diode material):

$$n = 1 \tag{14}$$

Based on the simplified conditions which given in Eqs. (12-14), now, we can formulate Eq. (6) so that the expression of the total current in the circuit is as follows [16, 17]:

$$I = I_l - I_0 \times \left(\exp\left(\frac{V + IR_S}{N_s V_{th}} \right) - 1 \right) \tag{15}$$

It can be concluded that a single-diode photovoltaic cell has 5 internal and external parameters. These parameters are reduced to 2 after simplification. However, for this reason, the equation representing the total current in the circuit is still nonlinear, and it is still very complicated to perform analysis only. We turned to programs to solve this problem, otherwise we did it with the help of mathematical programs that can avoid errors and avoid the complexity of analysis. In our work, we used the software package (PV*SOL 3.0 software packages), MATLAB software (Shell SQ150 PV module) , Mathcad2000 program, and Origin Lab 2019 program.

On the other hand, the output power curves are now easily given in terms of the total current of the PV cell as follows [16. 17]:

$$P = \left(\frac{V.I}{A_C} \right) = V. \left(\frac{I_l - I_0 \times \left(\exp\left(\frac{V + IR_S}{N_s V_{th}} \right) - 1 \right)}{A_C} \right) \tag{16}$$

Here, A_C is PV cell dimensions, (0.6 m^2).

3.3. Important parameters of solar cell

The most important of those parameters is the so-called open-circuit voltage V_{OC} (or Thévenin voltage) and it defines as the difference of electrical potential between two terminals of a device when disconnected from any circuit and the short-circuit current I_{SC} and it defines as the current passing through the solar cell when the voltage across the cell is zero. An important feature of solar cells is their ability to convert light into electrical energy. This is the so-called power conversion efficiency (PCE), which is the ratio of output power, which defines as the maximum output power of solar cells and it corresponds to the $I_{\max}$, namely, the maximum of current of cell to incident optical power P_{in} (in our study, $p_{in}\,(w/m^2)$. Therefore, the power conversion efficiency (PCE) is given by [19]:

$$PCE = \left(\frac{P_{\max}}{P_{in}}\right)\% \tag{17}$$

On the other side, the solar cell has a pivotal factor called the "fill factor", which is defined as the ratio of the maximum available power to the product of the open-circuit voltage and short circuit current as follows [20]:

$$FF = \left(\frac{V_{mas}.(\frac{I_{\max}}{A_c})}{V_{OC}.(\frac{I_{SC}}{A_c})}\right) = \frac{P_{\max}}{V_{OC}.(I_{SC}/A_c)} \tag{18}$$

Here, A_c is mentioned above.

3.4. Bias points, (I_{SC} ,odel) mV_{OC}

The curves of *(I-V)* can theoretically be expressed through a proposed characterization model expressing the behavior of current density in terms of voltage in the region where the current density behavior decreases linearly with the potential difference and also in the region where the current density decreases as a function of voltage sharply. According to this theoretical model, the current density expressed as a potential difference is as follows [20, 21]:

$$I = I_{SC}\left(1-(AV^{B})\right)-A_c(CV) \tag{19}$$

Here, *A, B* and *C* represent the parameters of the model. Within the components of Eq. (19), there is the linear region expressed in the $-A_cCV$ part (ohmic region). The effect in the ohmic region attributed to the shunt resistance and also Eq. (19) includes the non-linear region or so-called Space-charge-limited conduction, (SCLC region) expressed in the $I_{SC}\left(1-(AV^{B})\right)$ part [20. 21]. Relatedly, according to this model, one can calculate the output power, *p* of the solar cell as a function of the potential difference between its two ends as follows [20, 21]:

$$P = (I/A_c)V = [I_{SC}\left(1-(AV^{B})\right)-A_cCV]V \tag{20}$$

In order to avoid any complicated analysis when extracting the parameters of the present characteristic model, the bias points should be determined very accurately, so we choose the bias points to correspond to these points: I_{SC} , V_{OC} , $0.72I_{SC}$ $:(I_1,V_1)$ and $0.3V_{OC}$ $:(I_2,V_2)$. The mentioned parameters are given in the following equations [20. 21]:

$$C = \left(\frac{I_{SC} - I_2}{A_c \times 0.3V_{OC}} \right) \tag{21}$$

$$B = \frac{\log[(I_{SC} / A_c) - C V_{OC}) \Big/ ((I_{SC} / A_c) - (I_1 / A_C) - CV_1)]}{\log(V_{OC} / V_1)} \tag{22}$$

$$A = \left(\frac{\{(0.3V_{OC}) - V_1\} - (0.3V_{OC} \times 0.72.I_{SC} / A_c) + (V_1 \times I_2 / A_c)}{(I_{SC} / A_c)V_1.(0.3V_{OC}).\left((V_1)^{B-1} - (0.3V_{OC})^{B-1}\right)} \right) \tag{23}$$

Here, it must be distinguished that the *C* parameter plays a conductive role in the ohmic region, and the two parameters *B* and *A* are responsible for the steepness in the Space-Charge Limited Conduction SCLC region.

3.5. Extraction of parasitic resistances for solar cell

By dissipating the power in the resistor, the impact of resistance in the solar cell can reduce its efficiency. Common parasitic resistances are series resistance, R_{s0} which is accountable for the lowering of the output voltage in the voltage source region of I-V plotting, and parallel (shunt) resistance, V plotting in the current- which lowers the output current of the IR_{sh0} source region.

At the point where the current density is zero, namely, at $I = 0$, the series resistance R_{s0} is computed from the following formula [22]:

$$R_{s0} = \left(\frac{\partial V}{\partial I} \right)_{I=0} = [A_c C + A.B.I_{SC}.(V_{OC})^{B-1}]^{-1} \tag{24}$$

Similarly, at the point where the voltage is zero, namely, at $V = 0$, the shunt resistance R_{sh0} is extracted from the following equation [22]:

$$R_{sh0} = \left(\frac{\partial V}{\partial I} \right)_{V=0} = \frac{1}{A_c C} \tag{25}$$

4. Results and discussion

This work focuses on the simulation models mentioned in the above section by extracting the parameters of these models and then expressing the characteristics (current-voltage) and (power-voltage) characteristics of the CdS thin film in CdS/Si solar cells. One must be extremely careful when using the form to ensure that we enter the program data correctly to ensure that the results are right. These steps are indeed sufficient to obtain (current-voltage) characteristic curves, but in the future, efforts must be made to explore the influence of the internal parameters of the circuit (whether it is a single-diode system or a dual-diode system, or even a multi-diode) PV circuits.

Here, we divide the results into two subsections. The first section will deal with the results of the software package model. The second part is devoted to the model of bias point, and also this part discusses experimental measurement, that is, not through simulation models.

4.1. Results of using simulation software packages

4.1.1. (I-V) and (P-V) data as a function of temperature, T_c

Based on the simulation model called "PV* SOL 3.0 software package" [4], the (voltage-current) and (power-current) characteristics were simulated and performed (see Fig.2 and Fig. 3) for CdTe thin film in the hetero-junction of CdS/Si system. The conditions for simulating these characteristics here are that the solar radiation ($\Psi = 1000$ W/m^2) is constant, the absolute temperature of the diode varies from 25°C to 125°C, and the reference temperature is also 50°C. In all software processes, the reference solar radiation is constant at $\Psi^* = 1050$ W/m^2. The bias parameters in this case are summarized in Table 1. It can be clearly seen from Table 1 that the values of *PCE* and *FF* decrease with increasing temperature, which indicates that the increase in the temperature of the photodiode will reduce its efficiency if the temperature is too high, and this may cause its destruction and damage. All types of diodes and their use are affected by heat, because they are considered semiconductor devices, so the conductivity of semiconductors increases with temperature, so the current value also increases, but if the temperature rises too much, This will allow a large amount of current to flow, leading to a breakdown and in the end diode failure. It is very important to understand the role of temperature in the characteristics of diodes. Based on this knowledge, diodes can be used for many purposes, the most important of which is to choose the best LD for medical diagnosis of the eyes [5]. In solar cell systems, the open-circuit voltage is a factor that is commonly affected by temperature rise where the open-circuit voltage decreases with increasing temperature, while the short-circuit current also increases slightly. In our case, the open-circuit voltage is reduced due to the stability of the short-circuit current and the stability of solar radiation (irradiance).

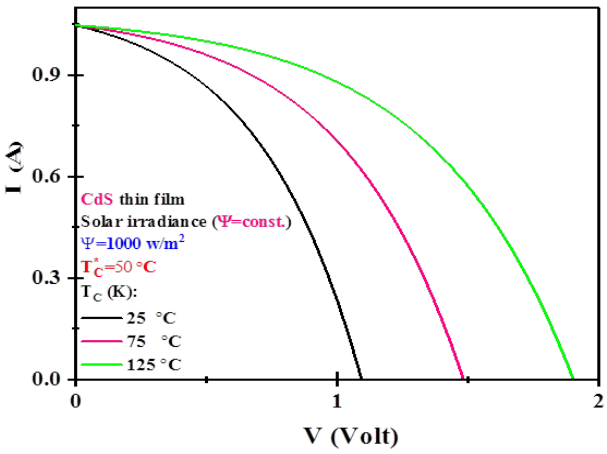

*Fig. 2. (I-V) characteristics of CdS/Si solar cell via PV*SOL 3.0 software packages: at various values of T_C.*

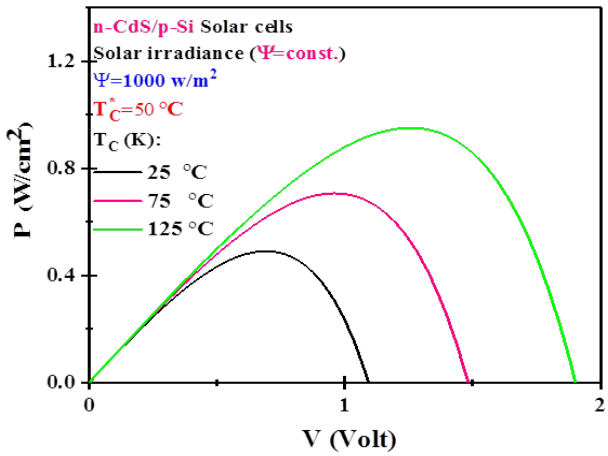

*Fig. 3. (P-V) characteristics of CdS/Si solar cell via PV*SOL 3.0 software packages: at various values of T_C.*

Looking at the current-voltage characteristic curves as a function of the surface temperature of the photovoltaic cell, we find that the voltage is more influenced by the temperature compared with the current. The bandgap value of the semiconductor declines as the interface temperature of the module rises, thus absorbing additional incident photon energy. As the temperature increases, the charge carriers increase significantly from valence to the conduction band, resulting in a slight rise in short-circuits current and saturated current also rises [25]. Here can be summed up a sentence that indicates that the PV module of the solar cell has the shortest current positive temperature coefficient in the circuit of the photovoltaic cell [26]. As the temperature rises; the heat-generated electrons accelerate the rate of phonon vibration, thereby suppressing the protection of electron holes. The electrons created in this way begin to adjust the electrical properties of the semiconductor, which results in a voltage drop in the end [27, 28]. Based on this explanation, it can be said that the PV modules of the solar cell have a negative temperature coefficient for the open voltage of the photoelectric circuit. Changes in open-circuit voltage and short circuit current with temperature are observed in published works cited in the corresponding references [25, 26, 29]. On the other side, from Table 1, one can notice that the fill factor *FF* of the photovoltaic module declines with rising temperatures. This result is consistent with the research performed by Fesharaki and his collaborators [30]. As well, we noticed from Table 1 that as the temperature of the module interface rises, the conversion efficiency of the array also drops. Due to this effect, the voltage and *FF* decline with rising temperatures. Therefore, the yielded power of the PV module is dropped, thereby lowering the efficiency of solar cell conversion. This behavior has been agreed with experimental results in the corresponding published works [28, 30, 31].

*Table 1. Yielded parameters for CdS/Si solar cell via PV*SOL 3.0 software packages: at various temperatures,.* T_C

T_C	Constants			Parameters of cell					
	T_C^*	Ψ	Ψ^*	I_{SC}	V_{OC}	$P_{\max}$	P_{in}	$PCE\,\%$	FF
(K)	(K)	(W/m^2)		A	V	(W/m^2)		Without unit	
298	323	1000	1050	1	1.900	1.25	20	6.25	65.78
348					1.485	0.96		4.8	64.64
448					1.098	0.68		3.4	61.93

4.1.2. (I-V) and (P-V) data as a function of the reference open-circuit voltage, V_{OC}^*

Fig. 4 and Fig. 5 show the (current-voltage) and (power-voltage) characteristics of the studied system as a function of the reference open voltage changes for PV cell. In this case, the simulation conditions are the constant temperature of the solar cell ($T_C = 25\ ^oC$), the reference temperature of the cell ($T_C^* = 25\ ^oC$), the constant of solar radiation ($\Psi = 1000$ W/m^2), and the constant of the reference solar radiation ($\Psi^* = 1050$ W/m^2). From the aforementioned Fig. 4 and Fig. 5, we notice that the opening voltage of the photoelectric circuit decreases with the increase of its reference opening voltage. The parameters of the PV cell in this case are summarized in Table 2. It can be seen from Table 2 that the *PCE* decreases while *FF* increases as the reference voltage increases.

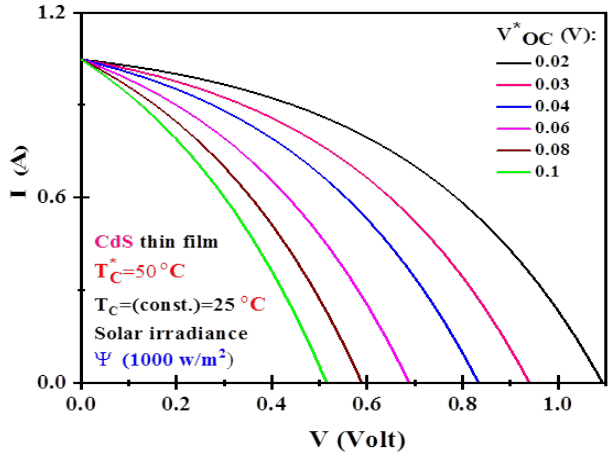

*Fig. 4. (I-V) characteristics of CdS/Si solar cell via PV*SOL 3.0 software packages: at various values of* V_{OC}^{*} .

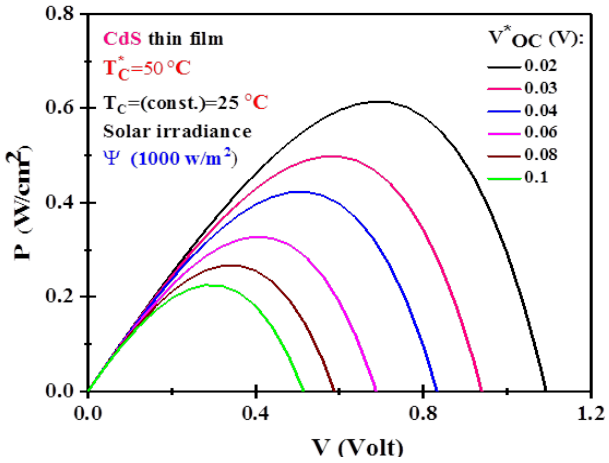

*Fig. 5. (P-V) characteristics of CdS/Si solar cell via PV*SOL 3.0 software packages: at various values of* V_{OC}^{*} .

*Table 2. Yielded parameters for CdS/Si solar cell via PV*SOL 3.0 software packages: at various values of reference open voltage,* V_{OC}^{*} .

V_{OC}^{*}	Constants				Parameters of cell					
	T_C	T_C^{*}	Ψ	Ψ^{*}	I_{SC}	V_{OC}	P_{max}	P_{in}	$PCE\,\%$	FF
V	(K)	(K)	(W/m^2)		A	V	(W/m^2)		Without unit	
0.02	298	323	1000	1050	1.045	1.09	0.70	20	2.95	61.45
0.03						0.94	0.59		2.5	60.06
0.04						0.83	0.50		2.05	57.64
0.06						0.69	0.41		1.6	56.86
0.08						0.59	0.32		1.1	51.90
0.1						0.51	0.22		2.95	41.27

4.1.3. (I-V) and (P-V) data as a function of the solar irradiance, Ψ

Figs. (6 and 7), respectively, highlight the characteristics of (current-voltage) and (power-voltage) as the solar radiation changes. In this case, the simulation condition is the stability of the solar cell temperature and its reference temperature, considering that the reference radiation (as described above) is a constant value in all cases where we use the software package program. It can be clearly seen from Fig.s 6 and 7 that as solar radiation increases, the open-circuit voltage and short circuit current of the solar cell both decrease. Table 3 lists the PV parameter values related to changes in solar irradiance. From the results in Table 3, it can be concluded that the *PCE* and *FF* values of solar cells decrease as the solar irradiance decreases. Therefore, we find that the more solar cells are exposed to more solar radiation, the higher their yield. On the other hand, the decrease in solar radiation matches the decrease in the open voltage of the PV circuit (see Table3). These results are consistent with the results performed by Naderi [25] and also this behavior was confirmed by Arjyadhara [26]. From Fig. 7, one can show that with solar irradiance decrease, the maximum power generated by the module declines. The change of power behavior with solar irradiance is consistent with Arjyadhara 's study [26] where he concluded that an increase in solar irradiance corresponds to an increase in the peak values of a curve power and vice versa in the event of diminution.

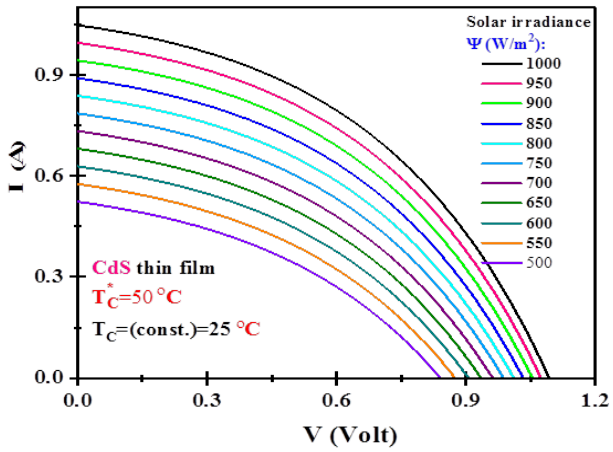

*Fig. 6. (I-V) characteristics of CdS/Si solar cell via PV*SOL 3.0 software packages: at various values of solar irradiance Ψ .*

*Table 3. Yielded parameters for n-CdS/p-Si solar cell via PV*SOL 3.0 software packages: at various values of solar irradiance, Ψ .*

Ψ	Constants			Parameters of cell					
	T_C	T_C^*	Ψ^*	I_{SC}	V_{OC}	P_{max}	P_{in}	$PCE\,\%$	FF
(W/m^2)	(K)	(K)	(W/m^2)	A	V	(W/m^2)		Without unit	
1000	298	323	1050	1.045	1.093	0.492	20	2.46	43.07
950				0.999	1.075	0.459		.2.29	42.74
900				0.948	1.057	0.423		2.11	42.21
850				0.893	1.036	0.386		1.93	41.72
800				0.841	1.014	0.355		1.77	41.62
750				0.789	0.989	0.322		1.61	41.26
700				0.738	0.964	0.291		1.45	40.90
650				0.683	0.936	0.261		1.31	40.82
600				0.631	0.908	0.229		1.12	39.96
550				0.581	0.879	0.201		0.10	39.35
500				0.528	0.844	0.174		0.09	39.04

4.4.2. Experimental curve and bias points, (I_{SC},) ModelV_{OC}

Fig. 8 and Fig. 9 result from laboratory procedures without using simulation software. Fig. 10 results from using a simulation program based on bias points taken from laboratory procedure curves. The consistency of Fig.s (8-10) data and output illustrate the accuracy of using the simulation model in this case. Table 4 and Table 5 summarize the parameters of photovoltaic cells when using experimental procedures and simulation models based on bias points. It is noted that as the PV cell temperature increases, the open-circuit voltage and short circuit current of the solar cell decrease. The yielded values of *PCE* and *FF* decrease with increasing temperature. This behavior is consistent with the work of Fesharaki at el. [30]. It can be seen from Table 5 that the performance of series resistance and parallel resistance depends on the speed of junction recombination. That is, these resistances increase with increasing temperature. In fact, when the recombination speed increases, the diode acts like a resistor, hindering the flow and passage of current [32-36]. The integration and interdependence in the properties of chalcogenide compounds, or those that contain at least a chalcogen element, or that are based in their synthesis on silicon and transitional elements, were received extensive studies, as the optical and electrical properties have been employed to determine the suitability of these systems for photovoltaic applications, especially for various uses in solar cells [37-42], optoelectronics [43-56], and electrodes [57-60]. Based on these studies, our current study was a link between the theoretical and experimental parts of the different system compositions of the studied solar cells.

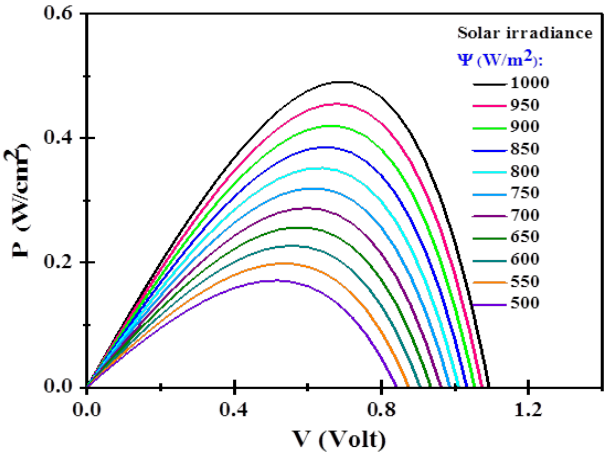

*Fig. 7. (P-V) characteristics of CdS/Si solar cell via PV*SOL 3.0 software packages: at various values of solar irradiance* Ψ .

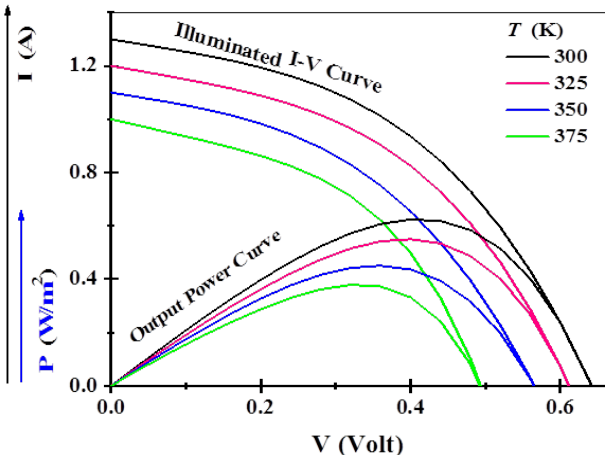

Fig. 8. (I-V) and (P-V) characteristics of CdS thin film in CdS/Si solar cell via bias points, (I_{SC},) V_{OC} model : at various temperatures.

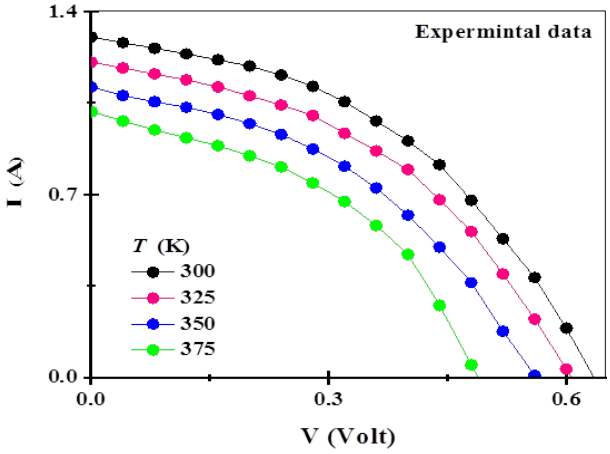

Fig. 9. (I-V) characteristics of CdS/Si solar cell via experimental steps: at various temperatures.

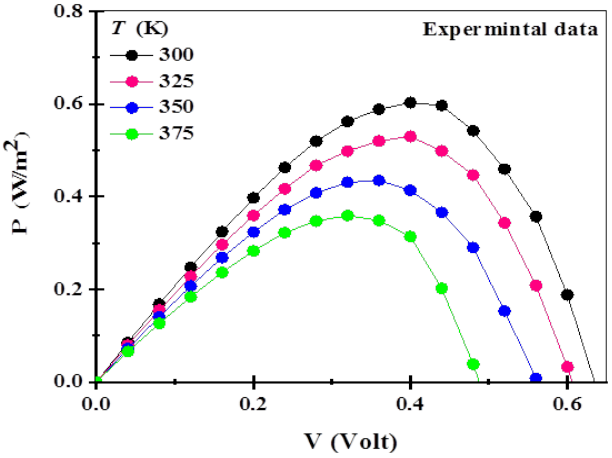

Fig. 10. (P-V) characteristics of CdS/Si solar cell via the experimental steps: at various temperatures.

Table 4. (I-V) characteristic experimental parameters of In/n-CdS/p-Si/Al at 300, 325, 350, and 375 K.

T (K)	**Experimental parameters**					
	***Voc* (V)**	***Isc* (A)**	$P_{max}\ (W/m^2)$	$P_{in}\ (W/m^2)$	$PCE\,\%$	***FF***
As-prep. (300)	0.67	1.3	0.628	20	3.14	72.10
325	0.63	1.21	0.541		2.71	70.96
350	0.57	1.1	0.44		2.2	70.17
375	0.5	1.01	0.353		1.76	69.90

Table 5. (I-V) parameters of In/n-CdS/p-Si/Al at 300, 325, 350, and 375 K.

T (K)	**Parameters of bias points modeling**														
	Isc	***I1***	***V1***	***Voc***	***I2***	***V2***	***A***	***B***	***C***	***Rs0***	***Rsh0***	P_{max}	P_{in}	$PCE\,\%$	***FF***
	(A)	**(A)**	**(V)**	**(V)**	**(A)**	**(V)**	Without unit			**(Ω)**		(W/m^2)		Without unit	
300	1.3	0.93	0.41	0.66	1.20	0.2	3.87	3.62	0.95	0.151	1.75	0.629	20	3.14	72.43
325	1.2	0.86	0.39	0.63	1.10	0.19	4.84	3.81	0.89	0.155	1.87	0.540		2.7	71.20
350	1.1	0.79	0.35	0.56	1.01	0.18	5.21	3.96	0.75	0.165	2.22	0.439		2.19	70.38
375	1	0.72	0.31	0.49	0.90	0.15	20.4	4.8	0.64	0.176	2.6	0.351		1.75	71.05

5. Conclusions

With the rise very dramatically in temperature, the output of solar cells will decline, primarily attributable to the rise in charge density, which contributes to a rise in the amount of inner carrier recombination. The constant high temperature will eventually damage the solar cells and destroy them. For these reasons, based on the simulation model, one can know how high the temperature should be, what the safety conditions are, and what the risks are caused by high temperature and solar irradiance. In this work, simulation models compatible with the experimental data have been used to finally achieve the purpose of extracting the parameters of the studied diode, thereby obtaining the (current-voltage) characteristic, and then the (power-voltage) curves. Besides, an in-depth understanding of the solar modules' power generation and how it changes with solar radiance and temperature would supply reliable data that is essential to the photovoltaic systems' size and design. Finally, in order to further simplify the simulation models and learn more about the current equations, more research about this side is needed.

Acknowledgments

The authors extend their appreciation to the Deanship of Scientific Research at King Khalid University, Saudi Arabia for funding this work through Research Groups Program under grant number RGP.1/239/43.

References

[1] Brano, V. L., Orioli, A., Ciulla, G., & Di Gangi, A., Solar Energy Materials and Solar Cells 94.8 (2010): 1358-1370; https://doi.org/10.1016/j.solmat.2010.04.003

[2] Mahmoud, Yousef, W. Xiao, and H. H. Zeineldin, IEEE transactions on Sustainable Energy 3.1 (2011): 185-186; https://doi.org/10.1109/TSTE.2011.2170776

[3] Chatterjee, Abir, Ali Keyhani, and Dhruv Kapoor, IEEE Transactions on Energy conversion 26.3 (2011): 883-889; https://doi.org/10.1109/TEC.2011.2159268

[4] Siddique, Hafiz Abu Bakar, Ping Xu, and Rik W. De Doncker, 2013 International Conference on Clean Electrical Power (ICCEP). IEEE, 2013; https://doi.org/10.1109/ICCEP.2013.6586957

[5] De Blas, M. A., Torres, J. L., Prieto, E., & Garcıa, A., Renewable energy 25.3 (2002): 371-380; https://doi.org/10.1016/S0960-1481(01)00056-8

[6] Angelis, L. De, et al., Characterization of n-CdS/p-Si heterojunction solar cells, Photovoltaic Solar Energy Conference. Springer, Dordrecht, 1981.

[7] Lu, Zhangbo, et al., Nanoscale 13.7 (2021): 4206-4212; https://doi.org/10.1039/D0NR09122G

[8] Al-Ani, Salwan K., Raid A. Ismail, and Hana F. Al-taay, Characterization of CdS: In/Si heterojunction solar cell, Iraq J. of Appl. Phys 1.2 (2005).

[9] Gao, Bing, et al., Solar Energy 173 (2018): 635-639; https://doi.org/10.1016/j.solener.2018.06.016

[10] Alaa, A., et al., 2014 IEEE 40th Photovoltaic Specialist Conference (PVSC). IEEE, 2014.

[11] Duan, Chunyan, et al., 2018 7th International Conference on Energy and Environmental Protection (ICEEP 2018). Atlantis Press, 2018; https://doi.org/10.2991/iceep-18.2018.260

[12] Cai, Lun, et al., Advanced Materials Interfaces 6.12 (2019): 1900367; https://doi.org/10.1002/admi.201900367

[13] Srivastava, Shalini, Shalini Singh, and Vineet Kumar Singh, Optical Materials 111 (2021): 110687; https://doi.org/10.1016/j.optmat.2020.110687

[14] Riad, A. S. Thin films, Solid 370: 253 (2000).| ll| Aly, AI, Akl, AA, Ibrahim, AA and Riad, AS, Egypt. J. Sol 24 (2001): 245; https://doi.org/10.1016/S0040-6090(99)00951-7

[15] Segura, A., Guesdon, J. P., Besson, J. M., & Chevy, A., Journal of applied physics 54.2

(1983): 876-888; https://doi.org/10.1063/1.332050

[16] Askarzadeh, Alireza, and Alireza Rezazadeh, Applied Energy 102 (2013): 943-949; https://doi.org/10.1016/j.apenergy.2012.09.052

[17] Wenham, S. R., Green, M. A., Watt, M. E., & Corkish, R., Applied Photovoltaics, Earthscan, London, UK (2007).

[18] Li, Y., Huang, W., Huang, H., Hewitt, C., Chen, Y., Fang, G., & Carroll, D. L., Solar Energy 90 (2013): 51-57; https://doi.org/10.1016/j.solener.2012.12.005

[19] Green, Martin A., Solar Cells 7.3 (1982): 337-340; https://doi.org/10.1016/0379-6787(82)90057-6

[20] Dash, D. P., Roshan, R., Mahata, S., Mallik, S., Mahato, S. S., & Sarkar, S. K., Journal of Renewable and Sustainable Energy 7.1 (2015): 013127; https://doi.org/10.1063/1.4909540

[21] Meir, S., Stephanos, C., Geballe, T. H., & Mannhart, J., Journal of Renewable and Sustainable Energy 5.4 (2013): 043127; https://doi.org/10.1063/1.4817730

[22] Patel, Sanjaykumar J., Ashish K. Panchal, and Vipul Kheraj, Journal of Nano-and Electronic Physics 5,№ 2 (2013): 02008-1.

[23] Rusirawan, Dani, and István Farkas. Electrotehnica, Electronica, Automatica 59.2 (2011): 9.

[24] Samer H. Zyoud, Atef Abdelkader, Ahed H. Zyoud. (2020), International Journal of Advanced Science and Technology, 29(06), 1167 - 1180.

[25] Tobnaghi, Davud Mostafa, and Daryush Naderi, Extensive Journal of Applied Sciences 3.2 (2015): 39-43.

[26] Arjyadhara, Pradhan, S. M. Ali, and Jena Chitralekha, International Journal of Engineering and Computer Science 2.1 (2013): 214-220.

[27] Dubey, Swapnil, Jatin Narotam Sarvaiya, and Bharath Seshadri, Energy Procedia 33 (2013): 311-321; https://doi.org/10.1016/j.egypro.2013.05.072

[28] Tobnaghi DM, Madatov R, Naderi D., International Journal of Advance Research in Electrical, Electronics and Instrumentation Engineering. 2013;2:6404-07.

[29] Ugwuoke, P. E., and C. E. Okeke, International Journal of Applied Science and Technology 2.3 (2012): 319-327.

[30] Fesharaki, V. Jafari, et al., Proceedings of the 1stInternational Conference on Emerging Trends in Energy Conservation-ETEC, Tehran, Iran. 2011.

[31] Razak, A., Irwan, Y. M., Leow, W. Z., Irwanto, M., Safwati, I., & Zhafarina, M. International Journal on Advanced Science, Engineering and Information Technology 6.5 (2016): 682-688; https://doi.org/10.18517/ijaseit.6.5.938

[32] Sari-Ali, I., B. Benyoucef, and B. Chikh-Bled, Journal of Electron Devices 5 (2007): 122-126.

[33] Assem, E. E., et al., Chalcogenide Letters 19.11 (2022); https://doi.org/10.15251/CL.2022.1911.825

[34] Alqahtani, A., et al., Optical Materials 134 (2022): 113055; https://doi.org/10.1016/j.optmat.2022.113055

[35] Qasem, Ammar, et al., Journal of Alloys and Compounds 899 (2022): 163374; https://doi.org/10.1016/j.jallcom.2021.163374

[36] Qasem, Ammar, et al., Optical Materials 122 (2021): 111746; https://doi.org/10.1016/j.optmat.2021.111746

[37] Qasem, Ammar, et al., Optical Materials 122 (2021): 111746; https://doi.org/10.1016/j.optmat.2021.111746

[38] Qasem, Ammar, et al., Applied Physics A 127.11 (2021): 1-13; https://doi.org/10.1007/s00339-021-04999-4

[39] Alshahrani, B., et al., Journal of Electronic Materials 50.8 (2021): 4586-4598; https://doi.org/10.1007/s11664-021-08989-3

[40] Elsaeedy, H. I., et al., Optics & Laser Technology 141 (2021): 107139; https://doi.org/10.1016/j.optlastec.2021.107139

[41] Elsaeedy, H. I., et al., Journal of Alloys and Compounds 867 (2021): 159150;

https://doi.org/10.1016/j.jallcom.2021.159150
[42] Qasem, Ammar, et al., Physica Scripta 98.1 (2022): 015825; https://doi.org/10.1088/1402-4896/aca99e
[43] Alqahtani, A., et al., Optical and Quantum Electronics 55.1 (2023): 1-36; https://doi.org/10.1007/s11082-022-04222-5
[44] Alqahtani, A., et al., Optics & Laser Technology 156 (2022): 108459; https://doi.org/10.1016/j.optlastec.2022.108459
[45] AL-Maqate, Faisal G., et al., Optical Materials 131 (2022): 112719; https://doi.org/10.1016/j.optmat.2022.112719
[46] Qasem, Ammar, et al., Optics & Laser Technology 148 (2022): 107770; https://doi.org/10.1016/j.optlastec.2021.107770
[47] Qasem, Ammar, et al., Materials Chemistry and Physics 277 (2022): 125620; https://doi.org/10.1016/j.matchemphys.2021.125620
[48] Qasem, Ammar, et al., Journal of Materials Science: Materials in Electronics 33.4 (2022): 1953-1965; https://doi.org/10.1007/s10854-021-07400-5
[49] Qasem, Ammar, et al., Physica B: Condensed Matter 627 (2022): 413600; https://doi.org/10.1016/j.physb.2021.413600
[50] Ahmed, Moustafa, et al., Optical Materials 113 (2021): 110866; https://doi.org/10.1016/j.optmat.2021.110866
[51] Qasem, Ammar, et al., Optical Materials 109 (2020): 110257; https://doi.org/10.1016/j.optmat.2020.110257
[52] Qasem, Ammar, et al., Journal of Electronic Materials 49.10 (2020): 5750-5761; https://doi.org/10.1007/s11664-020-08347-9
[53] Qasem, A., et al., Chalcogenide Letters 17.6 (2020): 277-300; https://doi.org/10.15251/CL.2020.176.277
[54] Shaaban, E. R., et al., Applied Physics A 126.1 (2020): 1-10; https://doi.org/10.1007/s00339-019-3217-1
[55] Shaaban, E. R., et al., Acta Physica Polonica, A. 136.3 (2019); https://doi.org/10.12693/APhysPolA.136.498
[56] Shaaban, Essam R., et al., Optik 186 (2019): 275-287; https://doi.org/10.1016/j.ijleo.2019.04.097
[57] El-Deeb, A. S., A. M. Ismail, and M. Y. Hassaan, Optik 221 (2020): 165358; https://doi.org/10.1016/j.ijleo.2020.165358
[58] Ibrahim, Mohamed M., et al., Journal of the Australian Ceramic Society (2022): 1-12; https://doi.org/10.1007/s41779-022-00723-4
[59] Mnawe, Ied Mohammed, et al., Nveo-Natural Volatiles & Essential Oils Journal| NVEO (2022): 1617-1632; https://doi.org/10.14704/nq.2022.20.4.NQ22108
[60] Shreif, A., et al., Ceramics International (2022); https://doi.org/10.1016/j.ceramint.2022.10.020